

---

This is an electronic reprint of the original article.  
This reprint may differ from the original in pagination and typographic detail.

Gronoff, Guillaume; Rahmati, Ali; Simon Wedlund, Cyril; Mertens, Christopher J.; Cravens, Thomas E; Kallio, Esa

## The precipitation of keV energetic oxygen ions at Mars and their effects during the comet Siding Spring approach

*Published in:*  
Geophysical Research Letters

*DOI:*  
[10.1002/2014GL060902](https://doi.org/10.1002/2014GL060902)

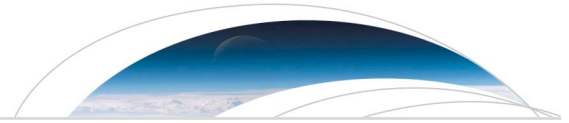
Published: 01/01/2014

*Document Version*  
Publisher's PDF, also known as Version of record

*Please cite the original version:*  
Gronoff, G., Rahmati, A., Simon Wedlund, C., Mertens, C. J., Cravens, T. E., & Kallio, E. (2014). The precipitation of keV energetic oxygen ions at Mars and their effects during the comet Siding Spring approach. *Geophysical Research Letters*, 41(14), 4844-4850. <https://doi.org/10.1002/2014GL060902>

---

This material is protected by copyright and other intellectual property rights, and duplication or sale of all or part of any of the repository collections is not permitted, except that material may be duplicated by you for your research use or educational purposes in electronic or print form. You must obtain permission for any other use. Electronic or print copies may not be offered, whether for sale or otherwise to anyone who is not an authorised user.



## RESEARCH LETTER

10.1002/2014GL060902

## Key Points:

- The O<sup>+</sup> pickup ions fluxes from the comet Siding Spring are computed
- The increase of O<sup>+</sup> fluxes at Mars is large
- The O<sup>+</sup> precipitation will create an ionosphere at 110 km

## Correspondence to:

G. Gronoff,  
Guillaume.P.Gronoff@nasa.gov

## Citation:

Gronoff, G., A. Rahmati, C. S. Wedlund, C. J. Mertens, T. E. Cravens, and E. Kallio (2014), The precipitation of keV energetic oxygen ions at Mars and their effects during the comet Siding Spring approach, *Geophys. Res. Lett.*, 41, 4844–4850, doi:10.1002/2014GL060902.

Received 17 JUN 2014

Accepted 8 JUL 2014

Accepted article online 14 JUL 2014

Published online 28 JUL 2014

## The precipitation of keV energetic oxygen ions at Mars and their effects during the comet Siding Spring approach

Guillaume Gronoff<sup>1,2</sup>, Ali Rahmati<sup>3</sup>, Cyril Simon Wedlund<sup>4</sup>, Christopher J. Mertens<sup>1</sup>, Thomas E. Cravens<sup>3</sup>, and Esa Kallio<sup>4</sup>

<sup>1</sup>Science Directorate, Chemistry and Dynamics Branch, NASA Langley Research Center, Hampton, Virginia, USA,

<sup>2</sup>SSAI, Hampton, Virginia, USA, <sup>3</sup>Department of Physics and Astronomy, University of Kansas, Lawrence, Kansas, USA,

<sup>4</sup>Department of Radio Science and Engineering, Aalto University School of Electrical Engineering, Aalto, Finland

**Abstract** Comet Siding Spring C/2013 A1 will pass Mars on 19 October 2014, entailing particle and dust precipitation in the Martian upper atmosphere and a potential dust hazard for orbiters. An estimate of the flux of energetic O<sup>+</sup> ions picked up by the solar wind from the cometary coma is shown, with an increase of the O<sup>+</sup> flux above 50 keV by 2 orders of magnitude. While the ionization of Mars' upper atmosphere by precipitating O<sup>+</sup> ions is expected to be negligible compared to solar EUV-XUV ionization, it is of the same order of magnitude at 110 km altitude during the cometary passage, leading to detectable increases in ionospheric densities. Cometary O<sup>+</sup> pickup ion precipitation is expected to be the major nightside ionization source, creating a temporary ionosphere and a global airglow. These effects are dependent on the solar and cometary activities at the time of the encounter.

### 1. Introduction

On 19 October 2014, the Siding Spring C/2013 A1 comet will pass in the vicinity of Mars with a closest approach of ~130,000 km with a heliocentric distance of 1.40 AU [Schneider, 2013; Moorhead et al., 2014]. The coma of the comet may envelop Mars, leading to the precipitation of molecules, ions, and dust particles. Several questions are raised about the effects of this precipitation. For example, the dust from the comet may pose a danger to the operating orbiters [Ye and Hui, 2014], i.e., Mars Odyssey, Mars Express (MEX), Mars Reconnaissance Orbiter, Mars Orbiter Mission, and Mars Atmosphere and Volatile Evolution (MAVEN). It will create shooting stars, observable from the surface of the planet [Selsis et al., 2005; Moorhead et al., 2014; Vaubaillon et al., 2014; Tricarico et al., 2014; Ye and Hui, 2014], and will likely be responsible for the generation of an extra ionospheric layer [Molina-Cuberos et al., 2003; Whalley and Plane, 2010; Withers, 2012].

The most important atmospheric effect will be the precipitation of atoms/molecules/ions and especially atomic oxygen atoms and O<sup>+</sup> ions. Although the main gas forming the corona of comets is H<sub>2</sub>O, the ionization and excitation by impact of this molecule will hardly be differentiable from those of O, for which incidentally more data are available concerning its collision cross sections with other molecules. Moreover, the cometary coronal gas will be partially ionized and dissociated by the EUV-XUV solar flux. To understand the atomic and molecular precipitation effects during such an encounter, it is therefore necessary to evaluate the flux of the neutral gas ejected from the comet and to compute its composition after the dissociation/ionization. A first approximation has been given by Schneider [2013]: at the closest approach, a density of 100 H<sub>2</sub>O molecules per cm<sup>3</sup> is expected; since the relative speed between the comet and Mars is 56 km s<sup>-1</sup>, the resulting H<sub>2</sub>O flux is of the order of 5 × 10<sup>8</sup> cm<sup>-2</sup> s<sup>-1</sup>. In addition, the kinetic energy for an oxygen atom at 56 km s<sup>-1</sup> is about 260 eV. However, this first estimation of the energy of the precipitating O does not take into account the dissociation and ionization of the precipitating molecules and the ion pickup effects.

The present paper aims to improve on the current view of the Mars/comet Siding Spring pass by addressing these approximations. It shows for the first time an estimation of the flux of pickup O<sup>+</sup> ions at Mars originating from photodissociated H<sub>2</sub>O molecules from the comet Siding Spring. It also shows the first estimation of the extra ionization in the Martian upper atmosphere coming from the precipitation of these accelerated O<sup>+</sup> ions.

In section 2, the models used for the estimation of the O density, the O<sup>+</sup> acceleration, and the ionization in the upper atmosphere of Mars are presented. In section 3, the oxygen ion fluxes at Mars and the total ionization rates are shown and discussed.

## 2. The Model

To compute the effects of the energetic O<sup>+</sup> on the Martian environment, several steps are necessary with four physical models used sequentially. First, a cometary neutral/ion atmosphere model is used; it requires an estimation of the production of O by photodissociation of H<sub>2</sub>O and OH, provided by the *Aeroplanets* model. Then, an ion pickup model computes the ionization of O and its acceleration by the solar wind toward Mars. Finally, a heavy ion transport model, *Planetocosmics*, computes the ionization by the precipitating O<sup>+</sup> in the upper atmosphere of Mars. Each of these models is briefly described in the following sections.

### 2.1. The Aeroplanets Model

The *Aeroplanets* model [Gronoff *et al.*, 2011, 2012a, 2012b; Simon Wedlund *et al.*, 2011] computes the ionization and excitation of atmospheric species by photon, electron, proton, and cosmic ray impacts, including the effect of the transport of secondary particles. It is based on the Trans\* models, initially developed for the Earth [Lilensten *et al.*, 1990; Lummerzheim and Lilensten, 1994; Simon *et al.*, 2007] and adapted to Venus [Gronoff *et al.*, 2007, 2008], Mars [Witasse *et al.*, 2002, 2003; Simon *et al.*, 2009; Gronoff *et al.*, 2012a, 2012b], or Titan [Gronoff *et al.*, 2009a, 2009b], including several other modules such as a fluid model (Earth) or an emission model (all planetary atmospheres).

*Aeroplanets* is used to compute the photodissociation probabilities in the *Haser* model [Haser, 1957] and to compare the final ionization rates by O<sup>+</sup> with the ionization rates due to the solar EUV-XUV flux and the secondary (photo-)electrons.

### 2.2. The Comet Atmosphere Model

The comet's neutral coronal density can be estimated using the *Haser* model [Jackson *et al.*, 2009, and references therein], which gives the steady state spherical distribution of a parent molecule and its associated daughter products, assuming a uniform and isotropic outgassing of the parent molecule. The direct observation of cometary comae shows that these assumptions and the reconstructed densities from the *Haser* model are reasonably accurate [Ahearn, 1982; Bertaux *et al.*, 1998].

The number density  $n$  of H<sub>2</sub>O parent molecules is estimated as a function of the radial distance  $r$  from the comet using  $n(r) = \frac{Q}{4\pi r^2 v} \times \exp(-\frac{r}{v\tau})$ , where  $Q$  is the H<sub>2</sub>O production rate ( $\sim 10^{28} \text{ s}^{-1}$ ),  $v$  is the outflow velocity of the neutrals ( $\sim 1 \text{ km/s}$ ), and  $\tau$  the characteristic lifetime (photodissociation and photoionization) of H<sub>2</sub>O molecules.

An estimation of the O neutral density, which is used in the ion pickup model to compute the O<sup>+</sup> flux, is achieved by computing the photodissociation frequency (H<sub>2</sub>O → OH → O) as well as the photoionization frequency (O → O<sup>+</sup>). The H<sub>2</sub>O photodissociation frequency is of the order of  $2.8 \times 10^{-6} \text{ s}^{-1}$  for quiet solar conditions and  $3.1 \times 10^{-6} \text{ s}^{-1}$  for active solar conditions as computed by *Aeroplanets*. The OH dissociation frequency and the O ionization frequency, as computed by *Aeroplanets*, have approximately the same value corresponding to  $1.2 \times 10^{-7} \text{ s}^{-1}$  for quiet solar conditions and  $4.5 \times 10^{-7} \text{ s}^{-1}$  for active solar conditions.

The major uncertainty for the present study is the ejection rate  $Q$ , which varies significantly depending on the comet (mainly as a function of its nuclear structure and surface [Skorov *et al.*, 2011; Huebner *et al.*, 2006]). It has been estimated at  $10^{31} \text{ s}^{-1}$  for Hale-Bopp [Morgenthaler *et al.*, 2001],  $10^{29} \text{ s}^{-1}$  for Hyakutake [Biver *et al.*, 1999; Combi *et al.*, 1998], and  $10^{28} \text{ s}^{-1}$  for Churyumov-Gerasimenko near perihelion [Bertaux *et al.*, 2014]. Siding Spring is a Oort-cloud comet [Moorhead *et al.*, 2014] and is therefore likely to have a large  $Q$  value. For the present study, we use a conservative estimate of  $10^{28} \text{ s}^{-1}$  for the quiet solar conditions and  $3 \times 10^{28} \text{ s}^{-1}$  for the active solar conditions. H<sub>2</sub>O, O, and OH densities as computed by the *Haser* model in quiet and active solar conditions are presented in Figure 1; it shows that at 100,000 km from the nucleus, H<sub>2</sub>O molecules are nearly entirely dissociated into O for active solar conditions.

### 2.3. The Ion Pickup Model

#### 2.3.1. Principle

O<sup>+</sup> ions with kinetic energies up to 100 keV have been observed by the Phobos [McKenna-Lawlor *et al.*, 1993] mission and later interpreted as coming from hot-oxygen atoms escaping Mars, ionized, picked up by the

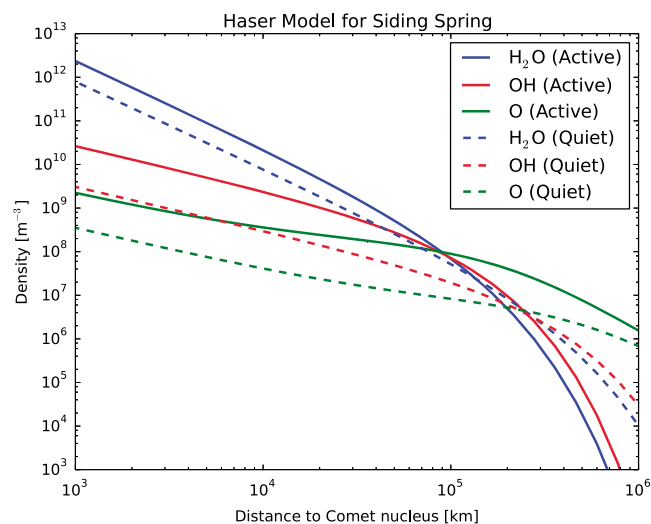


**Figure 1.** Haser neutral corona model for the comet Siding Spring for active and quiet solar conditions during its passage close to Mars.

computed on the dayside [Cravens *et al.*, 2002]. A first approximation, which is an upper estimate, is to consider these fluxes equal to the dayside ones.

### 2.3.2. Importance of Mass Loading

Solar wind mass loading is an important mechanism at comets with a sufficiently dense neutral corona that is continuously ionized by solar radiation and by the solar wind, resulting in the slowing down of the plasma flow on its approach to the cometary nucleus and possibly the formation of a cometary bow shock [Huebner *et al.*, 2006]. At large distances from the comet, newly produced cometary ions are picked up by the solar wind convection electric field, resulting in a net increase in their velocity. The supplementary kinetic energy is transferred from the solar wind to the cometary ions, and therefore, pickup ions may in turn slow down the solar wind [Jarvinen and Kallio, 2014]. Simultaneously, both solar wind magnetic and electric field intensities and geometries may be perturbed [Kallio and Jarvinen, 2012]. Two models are used to address the importance of the mass loading effects for the Siding Spring/Mars encounter. A 3-D self-consistent hybrid model is used to simulate mass loading around the cometary nucleus in the region  $x/y/z = [-30, 000\ 30, 000]$  km (see details in Kallio and Jarvinen [2012] and Jarvinen and Kallio [2014]). A simple 1-D gas dynamic model, based on the conservation of mass and momentum in the plasma flow, is used to analyze regions farther away from the comet's nucleus and assumes that a pickup ion instantaneously gets the speed of the ambient solar wind protons. In both models the total loss rate of  $H_2O$  is obtained from the Haser model. The maximum theoretical mass loading effect is studied by assuming that all the particles resulting from the destruction of  $H_2O$  molecules are ions, that is, that one water molecule produces ions with a total mass of 18 amu. The solar wind velocity is assumed to be  $U_{sw} = 600\text{ km s}^{-1}$ , the interplanetary magnetic field is  $(B_x, B_y, B_z) = (0, 5, 0)\text{ nT}$ , and the solar wind density is  $n_{sw} = 6\text{ cm}^{-3}$ . The slowing down of the solar wind at distances greater than  $\sim 30,000\text{ km}$  (4 times smaller than the cometary closest approach) from the nucleus is found to be only a few percent by this model.

Hybrid model runs show that mass loading effects do not need to be taken into account even closer to the nucleus. The solar wind is found to be unaffected until about 10,000 km from the comet's nucleus where the interplanetary magnetic field lines start to be distorted, forming a cone-shaped perturbation region with a near  $90^\circ$  aperture and expanding toward the antisolar point. Due to the geometry of the encounter and the relatively large closest approach to Mars of 130,000 km, this perturbation region will never intersect Mars' trajectory. Because the assumed loss rate of  $H_2O$  will certainly be revised at the time of the encounter, the simulated perturbation region might expand or contract accordingly. These results, assuming a large mass loading, show that the solar wind may be considered undisturbed in the pickup ion analysis.

### 2.3.3. The Pickup Ion Simulation

The position of the comet with respect to Mars at the closest approach is depicted in Figure 2. The ionization of the neutral coma of the comet will create  $O^+$  ions that are subsequently picked up by the solar wind. The

solar wind, and then reaccelerated toward Mars [Cravens *et al.*, 2002; Rahmati *et al.*, 2013, 2014]. A similar scheme happens to O atoms from the coma of comets [Cravens, 1989]. In the case of the passage of the comet Siding Spring, the density of cometary O is expected to be orders of magnitude higher than the Martian oxygen corona. Therefore, a large increase in high-energy  $O^+$  ions, picked up by the solar wind from the cometary coma, is expected.

Because of the interplanetary magnetic field,  $O^+$  pickup ions will have a gyro-radius large enough (about 20,000 km for our assumed values) to precipitate in the nightside upper atmosphere of Mars with fluxes similar to those com-

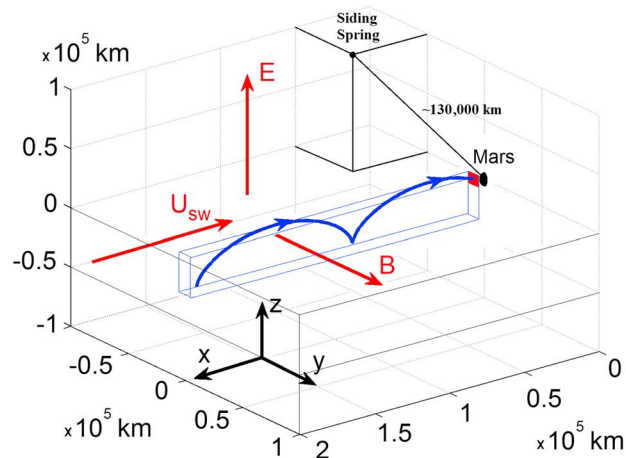


**Figure 2.** Cycloidal motion of an  $O^+$  pickup ion in the solar wind and crossing the sampling plane in red placed at 2000 km altitude. The  $x$  axis is sunward,  $z$  axis is normal to the ecliptic plane, and  $y$  axis completes the right-handed coordinate system. The blue box shows the simulation region for pickup ions that can cross the sampling plane. The positions of Mars and comet Siding Spring and the directions of the solar wind speed ( $U_{sw}$ ), the interplanetary magnetic field ( $B$ ), and the motional electric field ( $E = -U_{sw} \times B$ ) are also shown.

to collect the ions and record their kinetic energy when they cross the plane. Ions created outside of the simulation region will not cross the sampling plane. For a magnetic field perpendicular to the solar wind flow velocity, the maximum kinetic energy ( $E_{max}$ ) for the  $O^+$  ions is determined by  $E_{max} = 2 m U_{sw}^2$  where  $m$  is the mass of the ion.

#### 2.4. The Planetocosmics Model

The neutral atmosphere model for these observations comes from the Mars Climatology Database and is the one used in Norman et al. [2014]. The Planetocosmics model computes the cosmic rays deposition in planetary atmospheres [Desorgher et al., 2005; Gronoff et al., 2011; Sheel et al., 2012] and is based on the Geant4 library developed by the Centre Européen de Recherche Nucléaire (CERN). Planetocosmics computes

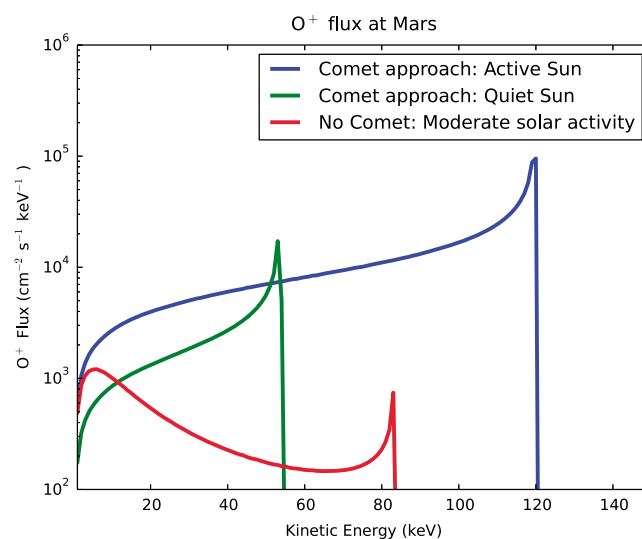


**Figure 3.** Flux of  $O^+$  pickup ions precipitating into the Martian upper atmosphere versus their kinetic energy. The simulation was made for active and quiet solar conditions during the passage of the comet and for moderate solar conditions without the comet (where  $O^+$  ions are picked up from the ionized neutral corona of Mars).

test particle code described in Cravens et al. [2002; Rahmati et al., 2014] is used to find the fluxes of  $O^+$  pickup ions near Mars.

A solar wind ( $U_{sw}$ ) speed of  $600 \text{ km s}^{-1}$  (respectively,  $400 \text{ km s}^{-1}$  and  $500 \text{ km s}^{-1}$  for the quiet and moderate solar conditions) and a magnetic field of  $5 \text{ nT}$  ( $4 \text{ nT}$  for the quiet and moderate solar conditions) perpendicular to the solar wind are assumed for the active solar condition following Ramati et al. [2013, 2014]. Therefore, in the following, the “solar condition” describes both the EUV-XUV flux and the solar wind speed.

The initial velocity of the pickup ions is assumed to be zero. As shown in Figure 2, the simulation region for tracking the trajectories of pickup ions is upstream of Mars, with a sampling plane placed at an altitude of 2000 km

to collect the ions and record their kinetic energy when they cross the plane. Ions created outside of the simulation region will not cross the sampling plane. For a magnetic field perpendicular to the solar wind flow velocity, the maximum kinetic energy ( $E_{max}$ ) for the  $O^+$  ions is determined by  $E_{max} = 2 m U_{sw}^2$  where  $m$  is the mass of the ion. The transport of  $O^+$  energetic ions down to relatively low energies (a hundred eV). It computes here the effect of the  $O^+$  ions precipitating in the upper atmosphere of Mars, following the same scheme as for the  $O^+$  flux at Titan [Gronoff et al., 2009a]. For the present simulations, we consider the ionization outside of the crustal magnetic field regions in order to neglect the magnetic shielding.

### 3. Results

The passage of the comet has two main effects on the energetic  $O^+$  ions at the vicinity of Mars. First,  $O^+$  fluxes may be greatly enhanced, leading to a drastic change in the plasma environment at Mars (composition, energy content) that may become a hazard for the instrumentation on board Martian orbiters [Bedingfield et al., 1996; Tahara et al., 1995; Tahara, 2003]. The

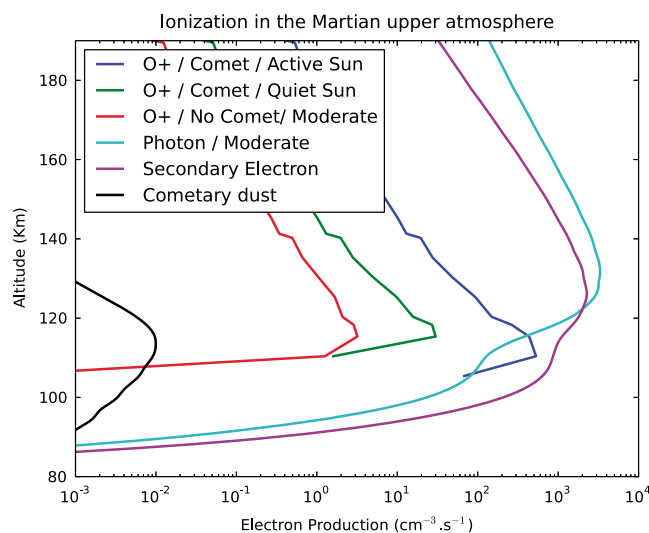


**Figure 4.** Ionization in the upper atmosphere of Mars due to the solar flux (photons and secondary electrons) for moderate solar activity, as compared with the O<sup>+</sup> ionization with and without the passage of the comet. The ionization by the cometary dust has been computed using the method of Molina-Cuberos et al. [2003], using a sporadic meteor background flux with a speed of 57 km s<sup>-1</sup> following Ye and Hui [2014].

model shows to a first approximation a flux proportional to the density of neutral oxygen O. Therefore, a higher H<sub>2</sub>O ejection rate Q will lead to a proportionally higher O<sup>+</sup> fluxes.

### 3.2. Ionization in the Upper Atmosphere of Mars

Figure 4 shows the electron production rate or ionization rate at Mars due to precipitating O<sup>+</sup>. This ionization rate is valid for dayside and is an upper limit for the nightside because Mars is a large obstacle for the O<sup>+</sup> flux at ionospheric altitudes. However, it could vary due to the shielding by local electric or magnetic fields. The ionization due to the comet peaks at an altitude of 110 km with a rate of  $6.0 \times 10^2$  electrons cm<sup>-3</sup> s<sup>-1</sup> for active solar wind conditions. This is 2 orders of magnitude above the ionization of 3 electrons s<sup>-1</sup> cm<sup>-3</sup> at 115 km altitude due to the Martian corona pickup ions and much higher than the quiet solar wind conditions of 30 electrons s<sup>-1</sup> cm<sup>-3</sup> at 115 km altitude. The ionization due to the comet during high solar activity is of the same order of magnitude as that due to the EUV-XUV flux: for a  $F_{10.7}$  value of 130 (moderate solar activity) and a solar zenith angle of 45°, this ionization is  $1.0 \times 10^3$  electrons cm<sup>-3</sup> s<sup>-1</sup>. When compared to the nightside ionization rates, the O<sup>+</sup> precipitation will dwarf all other sources, even the ionization by the dust from the comet on the side of the planet facing this meteor flux [Ye and Hui, 2014]. Since the ionization rate due to O<sup>+</sup> ion precipitation is comparable to the dayside ionization rate at 110 km, the electron density will also be comparable, of the order of  $1.0 \times 10^{4-5}$  cm<sup>-3</sup> [Withers et al., 2012a]. Such electron densities have been detected before: the precipitation of O<sup>+</sup> will therefore be noticeable with instruments such as Mars Advanced Radar for Subsurface and Ionosphere Sounding (on board MEX) [Gurnett et al., 2008] and radio occultation experiment (such as Mars Express Radio Science Experiment [Withers et al., 2012b] on board MEX). In addition, such a deposition of energy will create airglow emissions [Gronoff et al., 2012a] that may become the major emission in the UV on the nightside of Mars and are therefore likely to be observable by the Imaging Ultraviolet Spectrograph instrument on board MAVEN [Schneider, 2013, also personal communication] and the Spectroscopy for Investigation of Characteristics of the Atmosphere of Mars instrument on board MEX [Simon et al., 2009].

## 4. Conclusion

For the first time, the O<sup>+</sup> fluxes and ionization due to cometary pickup ions precipitating in a planetary atmosphere are computed. The model is applied to the passage of the comet Siding Spring near Mars in October 2014. The increase in fluxes and ionization is found to be important—by up to 2 orders of magnitude compared to the flux of O<sup>+</sup> pickup ion from the Mars upper atmosphere—and likely to be observable

second effect is that the high-energy O<sup>+</sup> ions may precipitate into the upper atmosphere, ionizing neutral molecules and creating a temporary ion layer.

### 3.1. Ion Oxygen Fluxes at Mars

Figure 3 shows the flux of the Siding Spring O<sup>+</sup> pickup ions near Mars for quiet and active solar conditions. For comparison, the flux of O<sup>+</sup> ions originating from the neutral oxygen exosphere of Mars is also plotted. The O<sup>+</sup> flux due to the comet is about 2 orders of magnitude higher than that of the Martian neutral exosphere for energies greater than ~50 keV. The solar energetic particles instrument on board the MAVEN spacecraft can detect O<sup>+</sup> ions with energies greater than ~70 keV [Rahmati et al., 2013, 2014]. The Analyzer of Space Plasmas and Energetic Atoms instrument on board MEX will be able to detect the O<sup>+</sup> fluxes below these energies. The pickup ion

by instruments on board the different orbiters at Mars, notably MEX and MAVEN. The estimation of these fluxes is necessary to better address the danger encountered by these space missions while orbiting in a very variable plasma environment. The present results fill a gap in the interpretation and the assessment of the risks for Martian orbiters: the O<sup>+</sup> fluxes at 100 keV energy are estimated to be of the same order of magnitude as of proton fluxes for standard solar energetic particle events [Norman *et al.*, 2014]. The O<sup>+</sup> flux hazard will be more easily addressed than the dust impact hazard.

The prediction of the ionization rates in the upper atmosphere of Mars will permit a better understanding of the different observations and suggests a close monitoring of the electron density at 110 km altitude by the different radio/radar experiments during the passage of the comet. The exact magnitude of the O<sup>+</sup> flux, and so the exact effects in terms of energetics and composition in the Martian environment, are found to be extremely dependent on the solar conditions and on the activity of the comet and therefore will be correctly estimated a few days before the actual passage.

### Acknowledgments

We thank Nick Schneider (LASP), Sona Hosseini (UC Davis), Arun Gopalan (SSAI/NASA LaRC), and Ryan Norman (NASA LaRC) for useful discussions. S.W. and E.K. thank Touko Haunia (FMI) for calculating the comet trajectory with respect to Mars. We dedicate this paper to our colleagues who are in charge of any instrument/mission that will be orbiting Mars in October 2014 and who are obviously extremely stressed at the time this paper is written.

The Editor thanks two anonymous reviewers for their assistance in evaluating this paper.

### References

- Ahearn, M. F. (1982), Spectrophotometry of comets at optical wavelengths, in *IAU Colloq. 61: Comet Discoveries, Statistics, and Observational Selection*, edited by L. L. Wilkening, pp. 433–460, Univ. of Arizona Press, Tucson, Ariz.
- Bedingfield, K. L., R. D. Leach, and M. B. Alexander (1996), Spacecraft system failures and anomalies attributed to the natural space environment, *NASA Ref. Publ. 1390*, National Aeronautics and Space Administration, Marshall Space Flight Center, Huntsville, Ala.
- Bertaux, J. L., J. Costa, E. Quémerais, R. Lallement, M. Berthé, E. Kyrölä, W. Schmidt, T. Summanen, T. Makinen, and C. Goukenleuque (1998), Lyman-alpha observations of comet Hyakutake with SWAN on SOHO, *Planet. Space Sci.*, *46*(5), 555–568, doi:10.1016/S0032-0633(97)00179-7.
- Bertaux, J. L., M. R. Combi, E. Quémerais, and W. Schmidt (2014), The water production rate of Rosetta target comet 67P/Churyumov-Gerasimenko near perihelion in 1996, 2002 and 2009 from Lyman  $\alpha$  observations with SWAN/SOHO, *Planet. Space Sci.*, *91*, 14–19, doi:10.1016/j.pss.2013.11.006.
- Biver, N., et al. (1999), Spectroscopic monitoring of comet C/1996 B2 (Hyakutake) with the JCMT and IRAM radio telescopes, *Astron. J.*, *118*(4), 1850–1872, doi:10.1086/301033.
- Combi, M. R., M. E. Brown, P. D. Feldman, H. U. Keller, R. R. Meier, and W. H. Smyth (1998), Hubble space telescope ultraviolet imaging and high-resolution spectroscopy of water photodissociation products in comet Hyakutake (C/1996 B2), *Astrophys. J.*, *494*(2), 816–821, doi:10.1086/305228.
- Cravens, T. E. (1989), Test particle calculations of pick-up ions in the vicinity of comet Giacobini-Zinner, *Planet. Space Sci.*, *37*(10), 1169–1184, doi:10.1016/0032-0633(89)90012-3.
- Cravens, T. E., A. Hoppe, S. A. Ledvina, and S. McKenna-Lawlor (2002), Pickup ions near Mars associated with escaping oxygen atoms, *J. Geophys. Res.*, *107*, 1170, doi:10.1029/2001JA000125.
- Desorgher, L., E. O. Flückiger, M. Gurtner, M. R. Moser, and R. Bütkofer (2005), Atmocomics: A Geant 4 code for computing the interaction of cosmic rays with the Earth's atmosphere, *Int. J. Mod. Phys. A*, *20*(29), 6802–6804, doi:10.1142/S0217751X05030132.
- Gronoff, G., J. Liliensten, C. Simon, O. Witasse, R. Thissen, O. Dutuit, and C. Alcaraz (2007), Modelling dications in the diurnal ionosphere of Venus, *A & A*, *465*, 641–645.
- Gronoff, G., J. Liliensten, C. Simon, M. Barthélemy, F. Leblanc, and O. Dutuit (2008), Modelling the Venusian airglow, *A & A*, *482*, 1015–1029.
- Gronoff, G., J. Liliensten, L. Desorgher, and E. Flückiger (2009a), Ionization processes in the atmosphere of Titan. I. Ionization in the whole atmosphere, *A & A*, *506*, 955–964.
- Gronoff, G., J. Liliensten, and R. Modolo (2009b), Ionization processes in the atmosphere of Titan. II. Electron precipitation along magnetic field lines, *A & A*, *506*, 965–970.
- Gronoff, G., C. Mertens, J. Liliensten, L. Desorgher, E. Flückiger, and P. Velinov (2011), Ionization processes in the atmosphere of Titan. III. Ionization by high-Z nuclei cosmic rays, *A & A*, *529*, 143.
- Gronoff, G., C. S. Wedlund, C. J. Mertens, M. Barthelemy, R. J. Lillis, and O. G. Witasse (2012a), Computing uncertainties in ionosphere-airglow models: II. The Martian airglow, *J. Geophys. Res.*, *117*, A05309, doi:10.1029/2011JA017308.
- Gronoff, G., C. Simon Wedlund, C. J. Mertens, and R. J. Lillis (2012b), Computing uncertainties in ionosphere-airglow models: I. Electron flux and species production uncertainties for Mars, *J. Geophys. Res.*, *117*, A04306, doi:10.1029/2011JA016930.
- Gurnett, D., et al. (2008), An overview of radar soundings of the martian ionosphere from the Mars express spacecraft, *Adv. Space Res.*, *41*(9), 1335–1346, doi:10.1016/j.asr.2007.01.062.
- Haser, L. (1957), Distribution d'intensité dans la tête d'une comète, *Bull. Acad. Roy. de Belgique*, *43*, 740–750.
- Huebner, W. F., J. Benkhoff, M.-T. Capria, A. Coradini, C. De Sanctis, R. Orosei, and D. Pralnik (2006), *Heat and Gas Diffusion in Comet Nuclei*, ESA Publ. Div., Noordwijk, Netherlands.
- Jackson, W. M., X. Yang, X. Shi, and A. L. Cochran (2009), The temporal changes in the emission spectrum of comet 9P/Tempel 1 after deep impact, *Astrophys. J.*, *698*(2), 1609–1619, doi:10.1088/0004-637X/698/2/1609.
- Jarvinen, R., and E. Kallio (2014), Energization of planetary pickup ions in the solar system, *J. Geophys. Res. Planets*, *119*(1), 219–236, doi:10.1002/2013JE004534.
- Kallio, E., and R. Jarvinen (2012), Kinetic effects on ion escape at Mars and Venus: Hybrid modeling studies, *Earth Planets and Space*, *64*(2), 157–163, doi:10.5047/eps.2011.08.014.
- Lilensten, J., D. Fontaine, W. Kofman, L. Eliasson, C. Lathuillere, and E. S. Oran (1990), Electron energy budget in the high-latitude ionosphere during Viking/Eiscat coordinated measurements, *J. Geophys. Res.*, *95*(A5), 6081–6092, doi:10.1029/JA095iA05p06081.
- Lummerzhim, D., and J. Liliensten (1994), Electron transport and energy degradation in the ionosphere: Evaluation of the numerical solution, comparison with laboratory experiments and auroral observations, *Ann. Geophys.*, *12*, 1039–1051.
- McKenna-Lawlor, S. M. P., V. Afonin, Y. Yeroshenko, E. Keppler, E. Kirsch, and K. Schwingenschuh (1993), First identification in energetic particles of characteristic plasma boundaries at Mars and an account of various energetic particle populations close to the planet, *Planet. Space Sci.*, *41*(5), 373–380, doi:10.1016/0032-0633(93)90071-9.
- Molina-Cuberos, G. J., O. Witasse, J.-P. Lebreton, R. Rodrigo, and J. J. López-Moreno (2003), Meteoric ions in the atmosphere of Mars, *Planet. Space Sci.*, *51*, 239–249, doi:10.1016/S0032-0633(02)00197-6.

- Moorhead, A. V., P. A. Wiegert, and W. J. Cooke (2014), The meteoroid fluence at Mars due to comet C/2013 A1 (Siding Spring), *Icarus*, 237, 13–21, doi:10.1016/j.icarus.2013.11.028.
- Morgenthaler, J. P., W. M. Harris, F. Scherb, C. M. Anderson, R. J. Oliverson, N. E. Doane, M. R. Combi, M. L. Marconi, and W. H. Smyth (2001), Large-aperture [O I] 6300 Å photometry of comet Hale-Bopp: Implications for the photochemistry of OH, *Astrophys. J.*, 563(1), 451, doi:10.1086/323773.
- Norman, R. B., G. Gronoff, and C. J. Mertens (2014), Influence of dust loading on atmospheric ionizing radiation on Mars, *J. Geophys. Res. Space Physics*, 119, 452–461, doi:10.1002/2013JA019351.
- Rahmati, A., J. A. Croxell, T. Cravens, S. Pothapragada, A. F. Nagy, and S. A. Ledvina (2013), Escape of hot oxygen atoms from the atmosphere of Mars, Abstract P21A-1704 presented at 2013 Fall Meeting, AGU, San Francisco, Calif., 9–13 Dec.
- Rahmati, A., T. E. Cravens, A. F. Nagy, J. L. Fox, S. W. Bougher, R. J. Lillis, S. A. Ledvina, D. E. Larson, P. Dunn, and J. A. Croxell (2014), Pickup ion measurements by MAVEN: A diagnostic of photochemical oxygen escape from Mars, *Geophys. Res. Lett.*, 41, doi:10.1002/2014GL060289.
- Schneider, N. (2013), Siding Spring Comet, paper presented at Mars Upper Atmosphere Network (MUAN) Spring Meeting, Boston, Mass.
- Selsis, F., M. T. Lemmon, J. Vaubaillon, and J. F. Bell (2005), Extraterrestrial meteors a martian meteor and its parent comet, *Nature*, 435, 581, doi:10.1038/435581a.
- Sheel, V., S. A. Haider, P. Withers, K. Kozarev, I. Jun, S. Kang, G. Gronoff, and C. S. Wedlund (2012), Numerical simulation of the effects of a solar energetic particle event on the ionosphere of Mars, *J. Geophys. Res.*, 117, A05312, doi:10.1029/2011JA017455.
- Simon, C., J. Liliensten, J. Moen, J. M. Holmes, Y. Ogawa, K. Oksavik, and W. F. Denig (2007), TRANS4: A new coupled electron/proton transport code—Comparison to observations above Svalbard using ESR, DMSP and optical measurements, *Ann. Geophys.*, 25, 661–673.
- Simon, C., O. Witasse, F. Leblanc, G. Gronoff, and J.-L. Bertaux (2009), Dayglow on Mars: Kinetic modelling with SPICAM UV limb data, *Planet. Space Sci.*, 57, 1008–1021.
- Simon Wedlund, C., G. Gronoff, J. Liliensten, H. Ménager, and M. Barthélemy (2011), Comprehensive calculation of the energy per ion pair or W values for five major planetary upper atmospheres, *Ann. Geophys.*, 29(1), 187–195, doi:10.5194/angeo-29-187-2011.
- Skorov, Y. V., R. v. Lieshout, J. Blum, and H. U. Keller (2011), Activity of comets: Gas transport in the near-surface porous layers of a cometary nucleus, *Icarus*, 212(2), 867–876, doi:10.1016/j.icarus.2011.01.018.
- Tahara, H. (2003), Degradation of spacecraft polymer films by charged particle irradiation and its influences on charging/discharging events, in *Proceedings of the 9th International Symposium on Materials in a Space Environment, 16–20 June 2003*, edited by K. Fletcher, pp. 655–660, ESA Publ. Div., Noordwijk, Netherlands.
- Tahara, H., L. Zhang, M. Hiramatsu, T. Yasui, T. Yoshikawa, Y. Setsuhara, and S. Miyake (1995), Exposure of space material insulators to energetic ions, *J. Appl. Phys.*, 78(6), 3719–3723, doi:10.1063/1.359951.
- Tricarico, P., N. H. Samarasingha, M. V. Sykes, J.-Y. Li, T. L. Farnham, M. S. P. Kelley, D. Farnocchia, R. Stevenson, J. M. Bauer, and R. E. Lock (2014), Delivery of dust grains from comet C/2013 A1 (Siding Spring) to Mars, *Astrophys. J. Lett.*, 787, L35, doi:10.1088/2041-8205/787/2/L35.
- Vaubaillon, J., L. Maquet, and R. Soja (2014), Meteor hurricane at Mars on 2014 October 19 from comet C/2013 A1, *MNRAS*, 439(4), 3294–3299, doi:10.1093/mnras/stu160.
- Whalley, C. L., and J. M. C. Plane (2010), Meteoric ion layers in the Martian atmosphere, *Faraday Discuss.*, 147, 349–368, doi:10.1039/c003726e.
- Witasse, O., et al. (2002), Prediction of a CO<sub>2</sub><sup>+</sup> layer in the atmosphere of Mars, *Geophys. Res. Lett.*, 29(8), 104-1–104-4, doi:10.1029/2002GL014781.
- Witasse, O., et al. (2003), Correction to “Prediction of a CO<sub>2</sub><sup>+</sup> layer in the atmosphere of Mars,” *Geophys. Res. Lett.*, 30(7), 1360, doi:10.1029/2003GL017007.
- Withers, P. (2012), How do meteoroids affect Venus’s and Mars’s ionospheres?, *EOS Trans. AGU*, 93, 337–338, doi:10.1029/2012EO350002.
- Withers, P., et al. (2012a), A clear view of the multifaceted dayside ionosphere of Mars, *Geophys. Res. Lett.*, 39(18), L18202, doi:10.1029/2012GL053193.
- Withers, P., M. O. Fillingim, R. J. Lillis, B. Häusler, D. P. Hinson, G. L. Tyler, M. Pätzold, K. Peter, S. Tellmann, and O. Witasse (2012b), Observations of the nightside ionosphere of Mars by the Mars Express Radio Science Experiment (MaRS), *J. Geophys. Res.*, 117(A12), A12307, doi:10.1029/2012JA018185.
- Ye, Q.-Z., and M.-T. Hui (2014), An early look of comet C/2013 A1 (Siding Spring): Breather or nightmare?, *Astrophys. J.*, 787, 115, doi:10.1088/0004-637X/787/2/115.